Quaternary Research (2024), **120**, 36–52
doi:10.1017/qua.2023.68

Research Article

Loess transportation surfaces in west-central Wisconsin, USA

Randall J. Schaetzl
Department of Geography, Environment, and Spatial Sciences, Michigan State University, East Lansing, MI 48823, USA

Abstract

The concept of a loess transportation surface portends that saltating sands deflate silt/dust and send them into suspension. This process continues until a topographic barrier stops the saltating sand, allowing loess deposits to accumulate downwind. This paper reports on loess transportation surfaces in west-central Wisconsin, USA. During the postglacial period, cold, dry conditions coincided with strong northwesterly winds to initiate widespread saltation of freely available sands, deflating any preexisting loess deposits. Large parts of the study area are transportation surfaces, and lack loess. Loess deposits were only able to accumulate at "protected" sites—downwind from (east of) topographic barriers, such as isolated bedrock uplands and the north-to-south flowing Black River. Loess in locations from these barriers is thicker (sometimes >5 m) than would be expected, and in places has even accumulated above preexisting loess deposits. For example, downwind (east) of the Black River, most of the low-relief landscape is covered with ≈40–70 cm of silty loess, even though it is many tens of kilometers from the initial loess source. Upwind of the river, on the transportation surface, the low-relief landscape is only intermittently mantled with thin, scattered deposits of silty-sandy eolian sediment, and generally lacks loess.

Keywords: Loess, Eolian sand, Saltation, Transportation surface, Wind shadow, Sand ramp, Permafrost

(Received 31 May 2023; accepted 6 November 2023)

INTRODUCTION

To develop loess deposits, a mechanism must first exist to form silt. Commonly, glacial grinding and eolian abrasion are assumed to be the most effective processes for silt production/generation (Smalley, 1966; Smalley and Vita Finzi, 1968; Gardner and Rendell, 1994; Assallay et al., 1998; Smith et al., 2002). That said, eolian abrasion has also been invoked as a mechanism of silt generation, for example, Amit et al. (2014). Next, the silt must be entrained/deflated from its resting place and brought into atmospheric suspension. Silt and dust in suspension are then subject to transportation processes and, finally, deposition as loess. Deflation, transportation, deposition—all of Earth's loess deposits have experienced these three processes, usually in this order, and sometimes more than once. This paper expands on this loess generation "pathway" for sites in Wisconsin, USA, although the findings are potentially applicable to loess in a variety of environments.

In a now-classic paper, Mason et al. (1999) demonstrated how topography can have a dramatic effect on the transportation and (eventual) distribution of silt/dust, both regionally and locally (Fig. 1). They defined a loess transportation surface as a landscape where saltating sand can assist in the deflation/mobilization of silt grains, as initially discussed by Bagnold (1941) and as observed by Nickling (1978), thereby facilitating the transportation of fine-grained dust particles. Very little loess is actually retained on such a transportation surface, as the saltating sand is so effective at (further) mobilizing any silt that may have been temporarily deposited there. Important to the efficacy of a loess transportation surface is its "sparsely vegetated" character; well-vegetated surfaces would act to protect silt from the impacts of saltating sand. According to the model, silt and dust that have been mobilized (or remobilized) by saltating sand will stay episodically in transit until some sort of topographic obstacle/barrier is encountered, which stops/traps the saltating sand but allows the silt to continue on, downwind, in suspension. Such obstacles or barriers may be deep valleys or high uplands, for example, Sweeney et al. (2005). As a result, relatively sand-poor deposits of loess often accumulate downwind of topographic obstacles. I acknowledge that silt can be deflated without the assistance of saltating sand, for example, Sweeney and Mason (2013), but if sand is present, the process may be more robust.

The loess transportation surface model (LTSM, my nomenclature) was a game-changer for geoscientists working on landscapes where loess deposits are variable in thickness and texture and where sand is freely available. It provided the theoretical framework necessary to explain why some areas lack loess, while areas in close proximity have thick deposits of loess, and why the boundary between the two can be very abrupt (such as a deep river valley or a high, narrow ridge). Its utility is worldwide and it continues to be a highly useful explanatory model for loess distributions at all scales (Vanmaercke-Gottigny, 1981; Sweeney et al., 2005; Nyland et al., 2018; Mason et al., 2019; Li et al., 2020; Bertran et al., 2021; Pötter et al., 2021; Schaetzl et al., 2021; Stevens et al., 2022; Wang et al., 2022), and even for dune sand (Loope et al., 2012; Shandonay et al., 2022; Wang et al., 2022).

The purpose of this paper is to provide data-rich, clear-cut examples of how the LTSM explains not only loess distributions

Corresponding author: Randall J. Schaetzl, Email: soils@msu.edu
Cite this article: Schaetzl RJ (2024). Loess transportation surfaces in west-central Wisconsin, USA. *Quaternary Research* **120**, 36–52. https://doi.org/10.1017/qua.2023.68

© The Author(s), 2023. Published by Cambridge University Press on behalf of Quaternary Research Center

https://doi.org/10.1017/qua.2023.68 Published online by Cambridge University Press

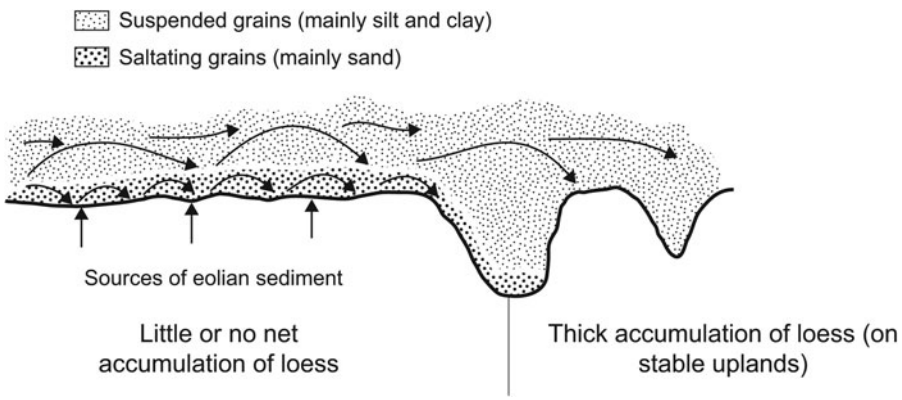


Figure 1. A reproduction of fig. 4 in the loess transportation surface paper by Mason et al. (1999).

across a landscape, but also loess textures and thicknesses. I do not intend this research to be so much an *affirmation* of the LTSM, or even a *test*. Rather, my approach is to use an extensive data set of loess thicknesses and textures, across and downwind of a transportation surface, to add theoretical depth and detail to the model. The data derive from a landscape of variable (but generally low) relief in west-central Wisconsin, USA, where sands are freely available, where loess sources are generally known, and where postglacial transport directions were fairly uniform. Thus, data from this landscape provide an excellent *application* of the LTSM, which may add to our understanding of loess deflation–transportation–deposition systems worldwide.

STUDY AREA

Most of the study area in west-central Wisconsin lies within Chippewa and Eau Claire Counties on the west, and Clark County on the east. Although this landscape is generally low relief, it nonetheless has some isolated hills of sandstone that rise sometimes as high as 40–60 m above the surrounding landscape.

Glacial sediments and history

As indicated by the Late Wisconsin terminal moraine, which spans the northern margins of the study area, only the northern part of the study area was glaciated during Marine Oxygen Isotope Stage 2 (MIS 2; Attig et al., 2011; Syverson and Colgan, 2011; Fig. 2). Earlier glaciers did, however, advance as far south as southeastern Chippewa County, and into northern and central Clark County and nearby areas (Hole, 1943; Clayton, 1991; Syverson, 2007). Sediment associated with the earliest of these glaciers, mapped within the Bakerville Member of the River Falls Formation, is found mainly in southern Clark County (Syverson and Colgan, 2011). Ice that deposited this sediment flowed south, out of the Lake Superior basin, leaving behind reddish-brown, sandy loam till that, in places, drapes sandstone uplands. Bakerville tills average 57–63% sand (Mode, 1976; Attig and Muldoon, 1989; Syverson, 2007). The age of this glacial advance has not been confirmed, but may date to MIS 6 or 8 (Syverson and Colgan, 2011).

Evidence for an Early Wisconsin, possibly MIS 4, glaciation in the study area exists as sediment within the Merrill Member of the Copper Falls Formation, south of the Late Wisconsin moraine. Stewart and Mickelson (1976) reported a ^{14}C date on organic material overlying this till that suggested an Early Wisconsin age. Tills of the Merrill Member are loam and sandy loam in texture, averaging 49–63% sand (Stewart, 1973; Attig and Muldoon, 1989; Mode, 1976; Syverson, 2007).

Late Wisconsin (MIS 2) ice was the last glacial advance into the study area, where it formed a wide, conspicuous, and hummocky end moraine (Attig and Clayton, 1993; Syverson and Colgan, 2011; Fig. 2). At this time, meltwater formed valley trains of sandy and gravelly outwash. Permafrost had developed on landscapes within ≈100 km of the ice margin and persisted, between ≈19 and 15 ka (Holmes and Syverson, 1997; Schaetzl et al., 2022). Sand wedges that formed during this interval point to dry, cold, windy conditions across the study area. Ventifacts and bouldery surface lag deposits, which are common on these same landscapes, also support the notion of cold, windy, erosive conditions across the study area during and after the Late Wisconsin advance (Johnson, 1986; Syverson, 2007; Schaetzl et al., 2018).

Eolian sediments and history

Across the study area, as well as to its west (upwind), sandy sediments are widespread. Three main sources of sand exist here: (1) isolated uplands of sandstone bedrock, most of which is quite friable and easily weathered and eroded (Mudrey et al., 1982); (2) glacial sediments south of the Late Wisconsin moraine, which only shallowly overlie sandstone in many locations (Fig. 2); and (3) glacial outwash, sourced from the Late Wisconsin ice sheet and carried south, through the study area, by meltwater streams. The largest valley train deposits of this kind are associated with the Chippewa River, which has several high, wide alluvial terraces formed in outwash (Faulkner et al., 2016). Other, smaller streams also carried outwash, most notably the Eau Claire and Black Rivers.

Broadly speaking, loess deposits in Wisconsin and the Upper Great Lakes region are very spatially variable both in thickness and in texture (Hole, 1950; Scull and Schaetzl, 2011; Jacobs et al., 2012; Schaetzl and Attig, 2013). Many areas of the state lack loess entirely, usually because they were below a glacial lake (or the glacier) or on an aggrading outwash surface during the main loess depositional interval. Other loess-free areas occur on steep slopes, and thus any prexisting loess cover has been removed by erosion, or (as is most applicable here) are on landscapes where (presumably) saltating sand has deflated any preexisting loess. Interestingly, many of these loess-free areas immediately abut areas with thick loess (Fig. 3). Explaining the great spatial variability in the loess cover—at any of a variety

https://doi.org/10.1017/qua.2023.68 Published online by Cambridge University Press

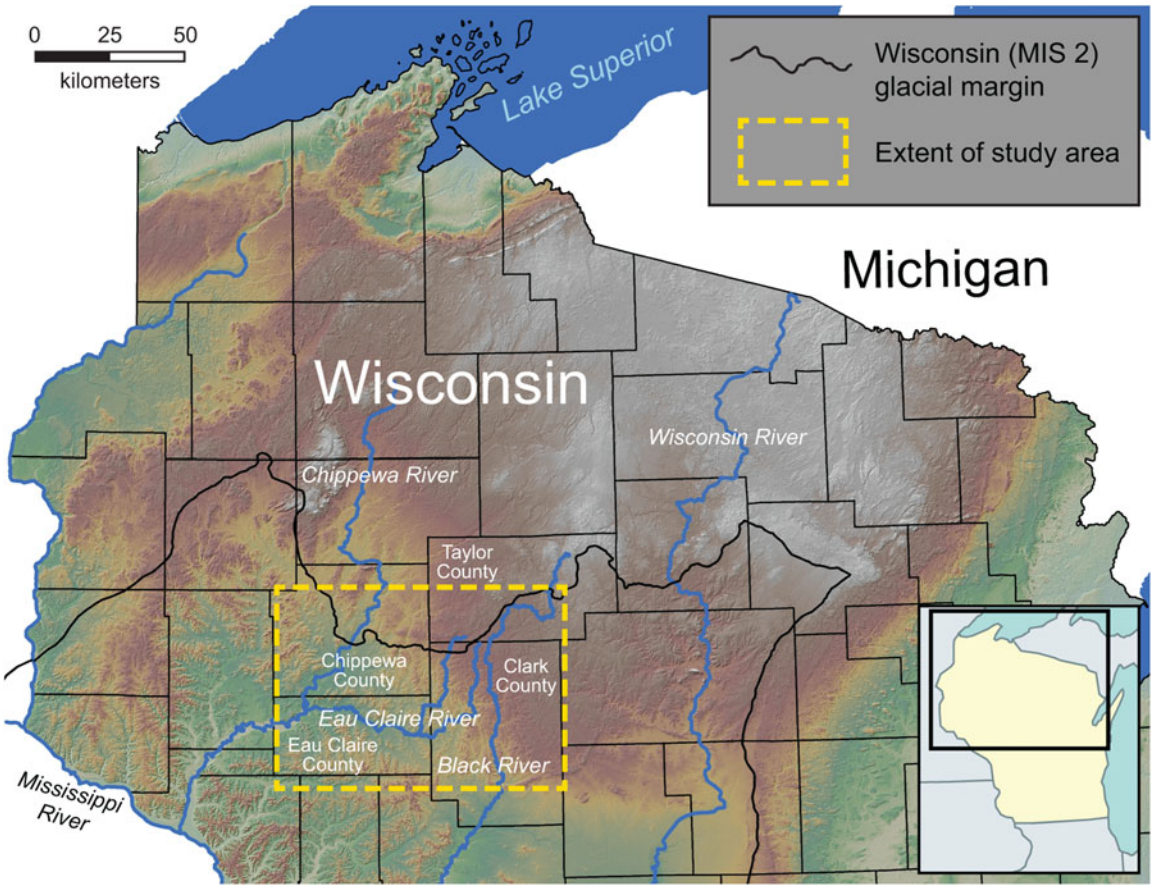


Figure 2. The regional setting for this study—northern Wisconsin, USA—showing the extent of Marine Oxygen Isotope Stage 2 (MIS 2; Late Wisconsin) glaciation, the major rivers that drain to the south across the region, and some county names.

of scales—has been a challenge for decades and was an impetus for this study.

Most of the loess in Wisconsin was derived from outwash surfaces (outwash plains and valley trains) and glacial lake plains formed during MIS 2, when the Laurentide Ice Sheet was retreating from the Upper Great Lakes region. Early researchers realized that this loess had generally been transported from west to east, as evidenced by the great thickness of loess deposits on the bluffs immediately east of the Mississippi River and other major, north-to-south flowing rivers (Hole, 1950; Ruhe, 1984; Bettis et al., 2003; Muhs et al., 2018). Spatial data on loess thickness and texture in southeastern Minnesota, just west of the study area, also indicate west-to-east transport of loess (Mason et al., 1994). Loess sources to the west of the Mississippi River floodplain were also important. For example, on uplands farther west, some of the preexisting loess was deflated and transported to Wisconsin (Mason et al., 1994; Jacobs et al., 2011; Schaetzl et al., 2018).

I delimited the major loess transportation surface in the study area based on its general lack of loess cover (Fig. 3). Sands are common both on and upwind of the transportation surface (Fig. 4). Low uplands on the otherwise low-relief transportation surface are typically mantled with till, bedrock residuum, or a thin cover of loamy sand- and sand-textured sediment that have an eolian history. And, as expected on a loess transportation surface, loess occurs in downwind areas, immediately beyond major topographic obstructions—in this case, best exemplified by the Black River valley (Fig. 3). The remainder of this paper explains in more detail the evidence for this area as a loess transportation surface and its impact on loess textures and distributions.

MATERIALS AND METHODS

Hole's (1950) map of eolian silt and sand deposits first identified—fairly accurately, given the scale of the map—the patchy nature of the loess across the study area. Additional detail on loess thickness and distribution was provided from Natural Resources Conservation Service (NRCS) county soil maps (Fig. 3). Data from these maps were downloaded from the NRCS's SSURGO/STATSGO2 Metadata site (https://www.nrcs.usda.gov/resources/data-and-reports/ssurgo/stats2go-metadata) and imported into a GIS. In the GIS, I rasterized the initial vector files and seamed the various coverages together into a raster mosaic. Using this data set, I next determined the parent material(s) for most of the soil series from the official series descriptions (OSDs) on the NRCS website (https://www.nrcs.usda.gov/resources/data-and-reports/official-soil-series-descriptions-osd). When the parent material description for a soil series was stated to be loess, usually over another sediment (or bedrock), loess thickness was gleaned from the OSD and entered into the GIS attribute table, using these thickness categories:

Loess > 152 cm (> 60 inches)
Loess = 102–152 cm (40–60 inches)
Loess = 51–102 cm (20–40 inches)
Loess = 25–51 cm (10–20 inches), and
Loess absent or < 25 cm (< 10 inches)

https://doi.org/10.1017/qua.2023.68 Published online by Cambridge University Press

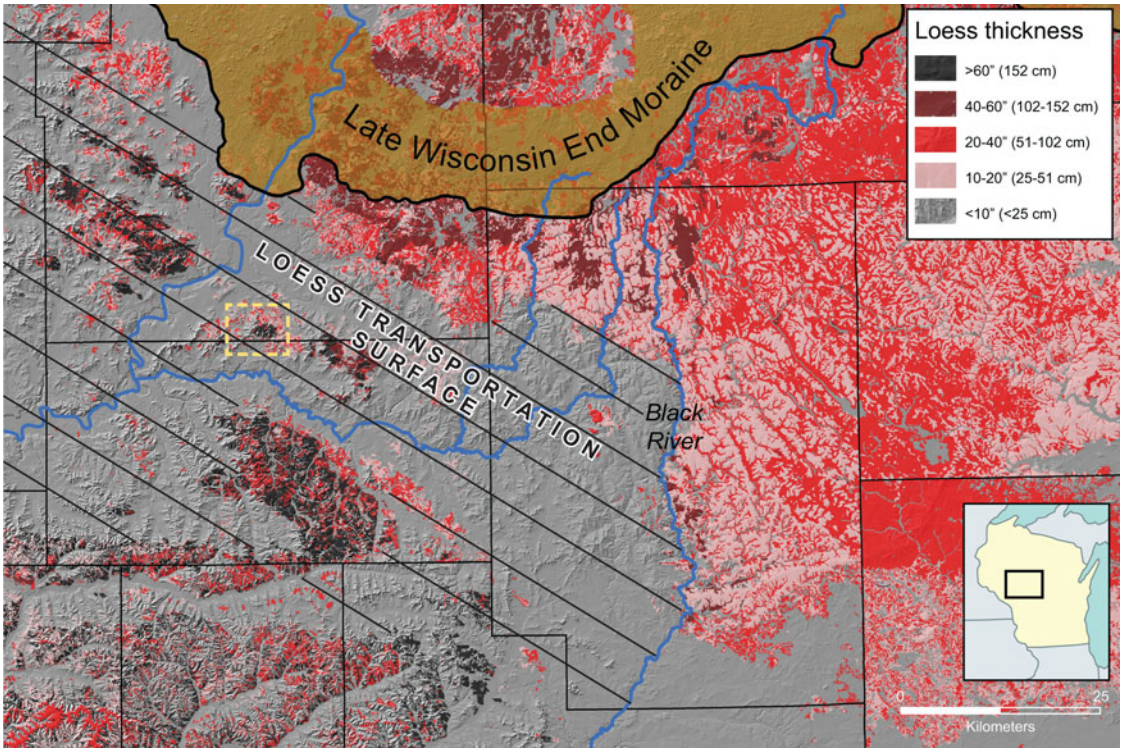


Figure 3. Loess deposits within the study area, as interpreted from the various county soil surveys of the Natural Resources Conservation Service (U.S. Department of Agriculture). Colors correspond to loess thicknesses. Gray areas, showing only the underlying hillshade digital elevation model (DEM), indicate areas that, according to the soil maps, lack a loess cover. As defined here, the extent of the loess transportation surface is shown, broadly, by diagonal lines. The inset box shows the extent of the landscape in this figure, on a small-scale map of the state of Wisconsin.

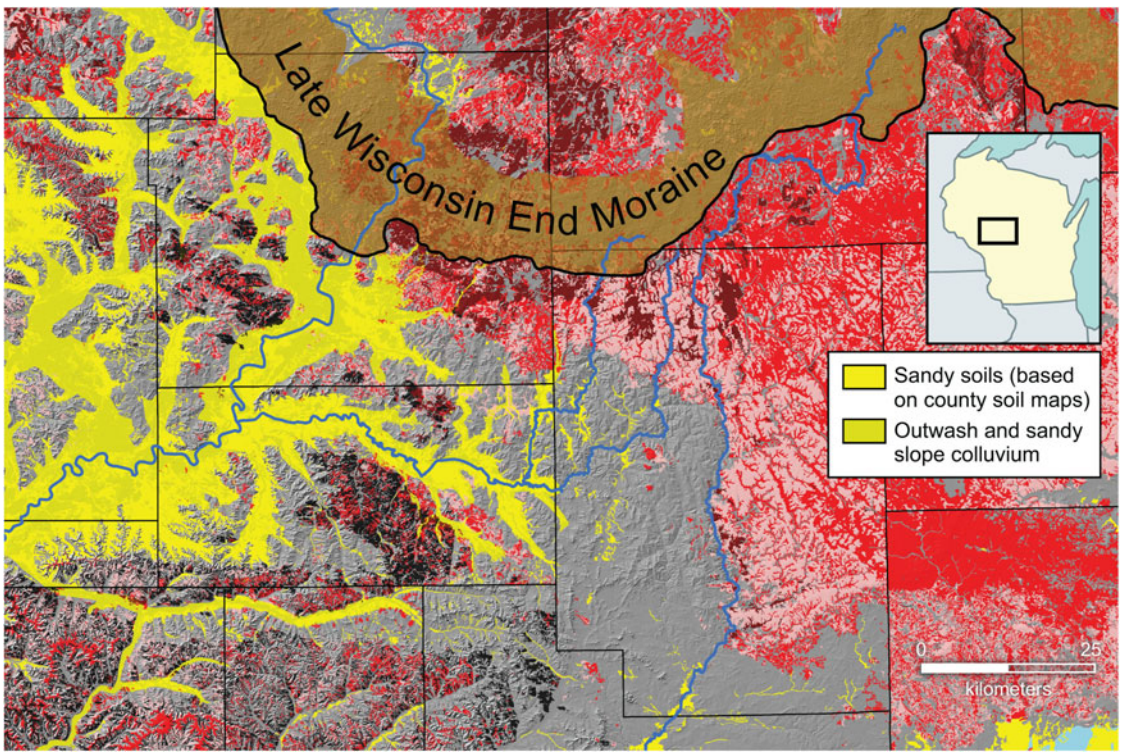


Figure 4. The extent of loess, glacial outwash, and sands within the study area and in areas farther west. Loess thickness symbology follows that in Fig. 3. Data derive from NRCS soil surveys.

https://doi.org/10.1017/qua.2023.68 Published online by Cambridge University Press

The data were then loaded onto a laptop computer equipped with a built-in GPS unit, thus facilitating field navigation to predetermined sites for sampling. Figure 3 provides the color legend used on these maps.

The first sampling goal was to obtain a large number of representative samples of eolian sediment from broad upland sites of low slope gradient, where loess was mapped, using a repeatable and consistent methodology. Stable, upland sites would have been most likely to retain loess by limiting erosion, redistribution, and/or burial. A digital elevation model (DEM) with 10 m resolution, used in conjunction with the soils data, helped to optimize potential sample targets. Forested areas were best, because they typically have never been plowed; agricultural fields were lower priority but were, necessarily, sampled in some areas.

Across the assumed loess transportation surface (Fig. 3), the goal was to obtain samples of whatever eolian sediment may exist on broad, stable uplands, where it would most likely have been preserved. After these types of sites were visited, samples were taken only if the sediment exhibited clear "eolian characteristics," such as the lack of coarse fragments and minimal amounts of coarse and very coarse sand; key to this identification, however, was the well-sorted nature of the sediment. Vegetation cover helped identify sites with an eolian mantle; sites that lacked such a cover were often in oak forest, being too sandy and coarse-textured for agriculture. Sites with a mantle of eolian sediment typically had a more mesic forest cover or were in cultivation. Almost always, below the lithologic contact between the eolian sediment (whether in the loess areas or on the transportation surface), the amount of coarser sands and gravels increased, making the field determinations relatively straightforward. At sites on stable uplands within the loess transportation surface where eolian sediment was not present, the site was noted in the GIS as such.

Spatially, the goal was for a relatively uniform sample grid. In areas of fairly uniform loess coverage, such as the loess-covered landscape east of the Black River (Fig. 3), the goal was for a sample density of one sample every ≈18–20 km^2. Nonetheless, in areas where loess thicknesses and textures changed rapidly over short distances, sample densities were much greater. For example, I sampled at high densities the thick loess that occurs to the east-southeast of several large sandstone uplands in the western part of the study area (Schaetzl et al., 2018).

In the field, at each of the several hundred sample sites, the thickness of the (presumed) eolian sediment was first determined in the field with a shovel and/or by hand auger. If the sediment was determined to be eolian in origin, a 500–600 g sample was then recovered and the thickness recorded. Because this work was performed mainly with a 195-cm-long hand auger, any site where the eolian sediment is thicker than 195 cm was recorded as 195 cm in the GIS. Because all sampling sites were located on stable uplands, all thicknesses should be viewed as maximum values; eolian sediment there would have experienced minimal erosion, as compared with adjacent, more sloping sites. The field-sampling goal was to obtain an amalgamated sample of eolian sediment that was representative of its entire thickness, while avoiding sampling the loess immediately above the underlying lithologic discontinuity. Loess and thin eolian deposits are often mixed with underlying sediment, especially in areas known to have had permafrost (McSweeney et al., 1988; Luehmann et al., 2013, 2016; Schaetzl and Attig, 2013; Schaetzl and Luehmann, 2013; Waroszewski et al., 2017, 2019). Thus, great care was taken to avoid sampling these mixed zones. Areas of obvious disturbance, for example, tree uprooting, were also avoided.

All samples were taken back to the laboratory, air-dried, lightly ground to pass a 2 mm sieve, and passed through a sample splitter two times, in order to achieve the homogeneity necessary for laser particle size diffraction on a Malvern Mastersizer 2000. From each loess sample, a small subsample was dispersed in a water-based solution of $(NaPO_3)_{13}$·Na_2O, after shaking for 10–15 min. As discussed in Miller and Schaetzl (2012), small subsamples analyzed in laser particle size analyzers are not always representative. Thus, I analyzed two subsamples from each sample and compared the data numerically. In cases where the suite of particle size data were sufficiently similar, I used the mean values for all subsequent data analyses. When the data from the two runs were sufficiently dissimilar (see Miller and Schaetzl [2012] for details), a third, or sometimes a fourth or fifth, subsample was run, and the two most comparable samples were used to generate the mean values used in subsequent analyses.

Finally, because of the assumed importance of sand and westerly winds on the transportation surface, I derived sand data from ≈2 kg samples taken from 17 sites across the region. These sites were (1) a gravel pit in the outwash deposits of the Chippewa River, (2) the sandy alluvium of the Eau Claire River valley, and (3) an upland on the transportation surface where the sediment was unmistakably eolian sand. After each sample was fully homogenized in the lab, I subsampled it and counted sand grains, forming two groups: (1) quartz and chert and (2) all others. The goal behind this grain-counting strategy was to generally differentiate light from heavy minerals within the sands.

RESULTS AND DISCUSSION

Much of the loess transportation surface identified in Figure 3 lacks a cover of eolian sediment of any kind, and where eolian sediment does occur, it is thin and patchy. Explaining this distribution, through application of the LTSM, is a goal of this paper. The LTSM requires that sand is available to deflate silt grains, and, of course, wind must also be strong enough to transport the sand. Finally, vegetation cover must be minimal enough that sand is exposed, making the land surface vulnerable to deflation. All of these preconditions exist (or once existed) within the loess transportation surface, as delineated in Figure 3.

Eolian transport directions and intensity

MIS 2 loess (Peoria Silt) is widespread across the upper Midwest and Great Plains of the United States (Bettis et al., 2003). Although most of the thick Peoria loess deposits are south of the study area, the same sediment can be traced up and into the study area, where it drapes uplands on both sides of the Mississippi River valley. Peoria Loess covers many areas that were also glaciated during MIS 2, implying that its deposition continued past the LGM (last glacial maximum) period, for example, Schaetzl and Hook (2008) and Jacobs et al. (2011).

Early researchers understood that loess deposits across the upper Midwest, most of which are associated with glacial meltwater, had been generally transported on westerly winds, based on spatial patterns of thickness and texture (Smith, 1942; Leighton and Willman, 1950; Fehrenbacher et al., 1965; Frazee et al., 1970; Ruhe, 1973; Rutledge et al., 1975; Hallberg, 1979; Olson and Ruhe, 1979; Putman et al., 1988; Mason et al., 1994). Both

https://doi.org/10.1017/qua.2023.68 Published online by Cambridge University Press

model data (COHMAP Members, 1988; Kutzbach et al., 1993; Conroy et al., 2019), as well as more recent work on eolian deposits (Muhs and Bettis, 2000; Mason, 2001; Bettis et al., 2003; Roberts et al., 2003; Mason et al., 2011; Muhs et al., 2013, 2018), have continued to support these early interpretations, while adding detail to knowledge of regional paleocirculation patterns. Exceptions occur, however, where evidence suggests an easterly paleowind component, although these instances are typically more "local" and are ascribed either to passing cyclones (Muhs and Bettis, 2000) or to katabatic winds off the ice sheet (Krist and Schaetzl, 2001; Schaetzl and Attig, 2013; Schaetzl et al., 2016). That is, a broadscale, regional pattern of *westerly wind*s at and near the LGM remains widely accepted for the study area.

Paleoclimate data for the study area in Wisconsin during and immediately after the LGM add even more detail to this overall picture. Modeled data indicate dry, cold conditions at the LGM (Bromwich et al., 2004), which is consistent with ground data showing permafrost at this time (Holmes and Syverson, 1997; Johnson, 1986; Clayton et al., 2001; French and Millar, 2014; Batchelor et al., 2019; Schaetzl et al., 2022). Winter was the windiest season (Bromwich et al., 2004).

In the following sections, I discuss two ways in which loess transportation surfaces may have functioned in the region: (1) short-distance transport up and over isolated bedrock knobs, associated with sand ramps; and (2) long-distance transport across low-relief surfaces. Both cases illustrate the utility of the model of Mason et al. (1999), explaining why loess deposition is often focused in areas downwind of a topographic obstruction.

Loess transportation systems I: the role of isolated, bedrock uplands

Within the study area, as in Iowa (Kerr, 2023), a variety of data are in strong agreement for postglacial eolian transport along a focused, west-northwest direction (Schaetzl et al., 2018). For example, long, narrow, sand stringers—not unlike small longitudinal dunes—on sandy surfaces to the immediate west of the study area, which have been interpreted as age-equivalent to loess, are nicely aligned WNW-ESE (Schaetzl et al., 2021; Shandonay et al., 2022). Sand ramps are also common on the western sides of bedrock uplands (Hanson et al., 2015; Schaetzl et al., 2021; Shandonay et al., 2022). The fairly uniform loess cover on the bedrock uplands in the far western parts of the study area adds to the interpretation of west-to-east transport of eolian siltloes. The loess is thickest and coarsest near the Mississippi River valley (a silt source). Although the loess thins gradually to the east, it uniformly covers the flat, table-like uplands near the river. Importantly though, this loess cover then becomes (locally) much thicker just *east* of the steep, bedrock escarpments that mark the eastern edge of the upland, as if the loess were preferentially accumulating in the "wind shadow" of the escarpment (Fig. 5).

However, the most convincing primary data that support the WNW-to-ESE transport of eolian sediment lies in the *local distribution* of loess deposits, relative to high, isolated bedrock knobs. Across the study area, loess is routinely absent on the west and northwest slopes of these ridges. Here, bedrock is often at the surface or covered by thin deposits of poorly sorted, sandy-silty regolith (Fig. 6A) or by sand ramps of well-sorted eolian sand. Thick loess occurs, however, on the east and southeast sides of these same ridges (Fig. 6B and C), and for some distance out and onto the lowlands beyond. The boundary between the area of nonexistent (or very thin) loess on the W-NW slopes versus the E-SE slopes is often very abrupt, and usually closely follows the ridgetop crest. (For the purposes of discussion, the W-NW slopes will hereafter be referred to as the windward slopes, and the E-SE slopes as the lee slopes.) This pattern is repeated on almost all of the isolated uplands in the region. Indeed, within the transportation surface landscape, loess usually only occurs (1) as scattered, thin deposits on the low-relief lowlands; and (2) in "protected" areas, such as in footslopes at the bottoms of narrow coves and ravines. The site shown in Figure 7 is a typical example of this relationship. Ridgetops in the study area are often mapped within the Northfield soil series, a Lithic Hapludalf that is described in the county soil survey as having bedrock at 41 cm (Thomas, 1977). Sideslopes and footslopes on the windward sides of the ridges are often mapped within the Elkmound soil series, a Typic Dystrudept whose offical series description also lists bedrock at 41 cm. Fieldwork in this area has repeatedly confirmed this relationship. At a number of sites along the windward slope of the ridge shown in Figure 7, field reconnaissance indicated thick deposits of eolian sand in coves and on toeslopes, but the backslopes were covered with only ca. 20–70 cm of loamy sediment overlying sandstone. I interpret these windward slopes as loess transportation surfaces, or sand ramps, incapable of retaining loess while winds were strong. Nonetheless, thick deposits of better-sorted, eolian sand were deposited and retained in protected areas at the bases of the slopes. Lower, smaller ridges, like the one in the southwest part of the landscape shown in Figure 7, were unable to "protect" lee sites, and hence they lack loess on all sides.

As shown in Figures 6 and 7, loess across the transportation surface is most common, and thickest, on the east and southeast sides of isolated bedrock knobs (Schaetzl et al., 2018). Indeed, field data across the study area indicate that sites with loess thicknesses >195 cm occur in only two types of locations: (1) on flat, stable ridgetops immediately downwind of the Mississippi River valley (an immediate loess source); and (2) in the lee of bedrock ridges (Fig. 5). Areas between the bedrock knobs are usually sandy and low relief, lacking loess entirely (Fig. 5). This pattern can be explained in two ways, both of which seem plausible; both follow the LSTM.

Scenario 1

In this scenario, during the main Peoria loess deposition interval, eolian silt being transported in from western sources was only able to accumulate on the sheltered, lee sides of ridges, because these same westerly winds generated clouds of saltating sand, deflated from outwash surfaces, exposed sandstone uplands, and sandy tills. This sand, transported up and around the windward slopes of bedrock knobs, helped mobilize the silt, preventing it from accumulating in all but the most topographically protected sites. Saltation would have ceased at the ridgetops, allowing loess (and some of the finest sands) to accumulate on their lee slopes and on lower relief sites downwind (Fig. 7). Thick deposits of eolian sand sometimes also accumulated in topographically preferred (protected) windward sites on bedrock slopes. To summarize, this scenario postulates that eolian silt and dust, entering the study area from western sources, was only able to persist on flat, bedrock-cored uplands in the west (which would have lacked sand for saltation), and in protected areas behind isolated sandstone uplands.

https://doi.org/10.1017/qua.2023.68 Published online by Cambridge University Press

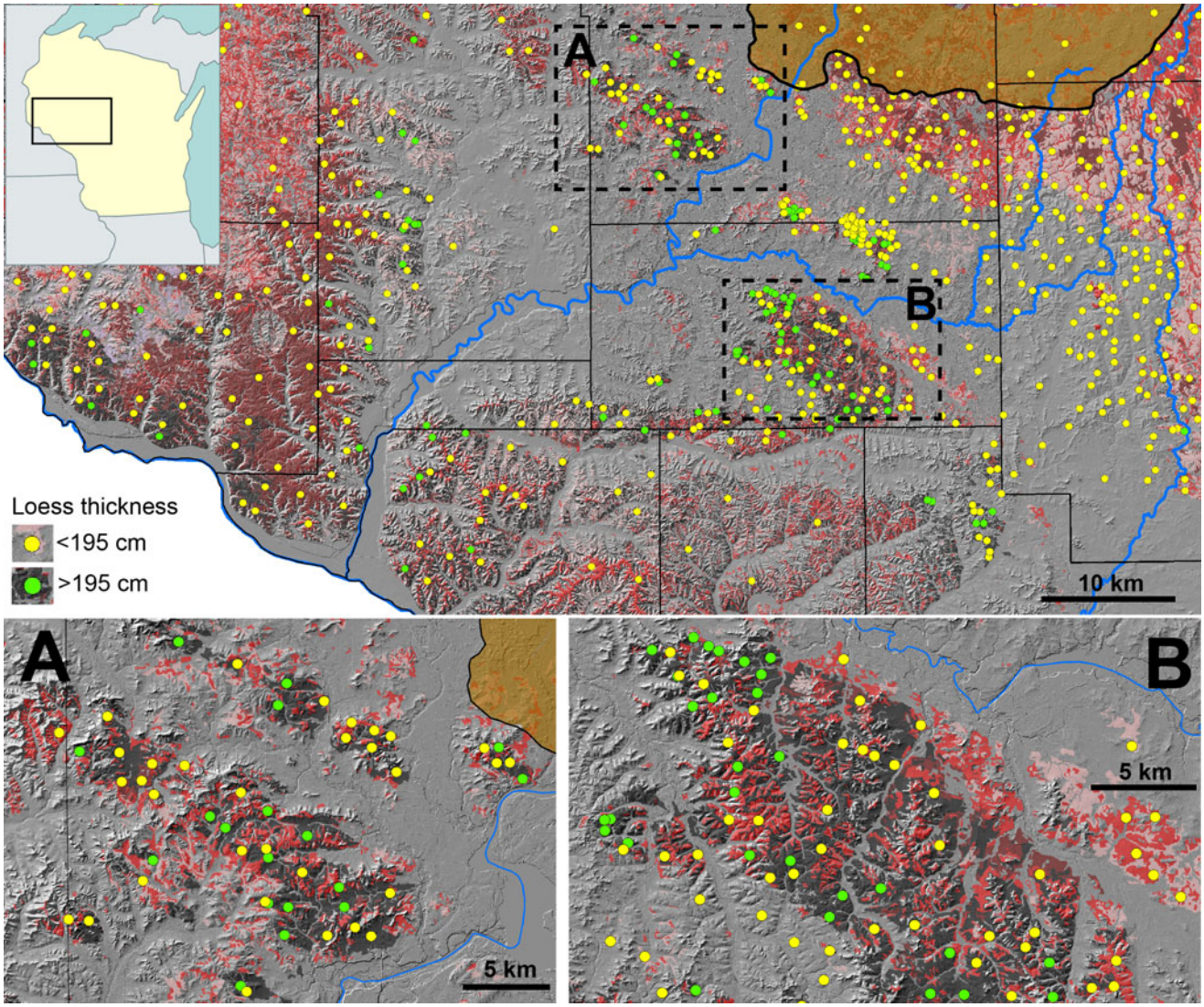


Figure 5. Maps of loess sample locations, symbolized by thickness categories, across western Wisconsin. Inset maps show detail for selected areas.

Scenario 2

In Scenario 2, loess was initially deposited broadly, across the landscape, but much of it was *later* remobilized and redistributed downwind. Saltating sand, sometimes accumulating in outwash valley trains as the ice sheet was melting, helped deflate, (re)mobilize, and *remove* this loess from unprotected areas. Just as in Scenario 1, eolian silt accumulated and persisted on the bedrock uplands in the western part of the study area, because these sites were well above (and upwind of) the main sand deposits of the central Chippewa Valley. The main difference on the ground occurs at "protected" sites within the transportation surface, where loess was not only preserved, but in some locations was buried by a second deposit of the "remobilized" loess.

Although both scenarios help explain the overall pattern of loess across the transportation surface, the model presented in Scenario 2 better fits the pattern seen on the ground, that is, where loess in the lee of many of the isolated bedrock ridges often exceeds 2 m in thickness, even though it is far from the (original) loess sources. Such an example occurs at the Geist farm orchard, in the immediate lee of a sandstone ridge (Fig. 8). Like other ridges on the loess transportation surface, the windward side of this ridge has only a minimal (less than ≈40 cm) cover of silty-sand regolith, while the lee side is blanketed with thick loess. Low-relief areas in lowlands near the ridge vary in loess cover, but seldom have more than ≈45 cm of loess, even as the thick (>195 cm) blanket of loess on the lee side of the ridge extends for ≈3 km downwind. Within this area of thick loess, but close to the ridge crest, I recovered a core, down to the sandstone bedrock at 585 cm. Grain-size data from the core provide insight as to the origins of loess at this site and to the two scenarios discussed earlier. In a thin zone immediately above the sandstone bedrock, the loess is sandy, as expected due to mixing of the earliest loess deposits with the underlying sandstone bedrock and its residuum (Fig. 9). Above that zone is ≈1.4 m of silt-rich loess with almost no sand. I interpret this as an earlier (i.e., the initial) loess deposit, formed by long-distance transport of silt in high suspension. Very little sand would have been transported at this time, perhaps due to weaker winds, widespread permafrost conditions, or a vegetation cover. The 1.4 m thickness would have been typical for loess in this area, taking into account the rate at which the loess cover thins across the low-relief bedrock uplands east of the

https://doi.org/10.1017/qua.2023.68 Published online by Cambridge University Press

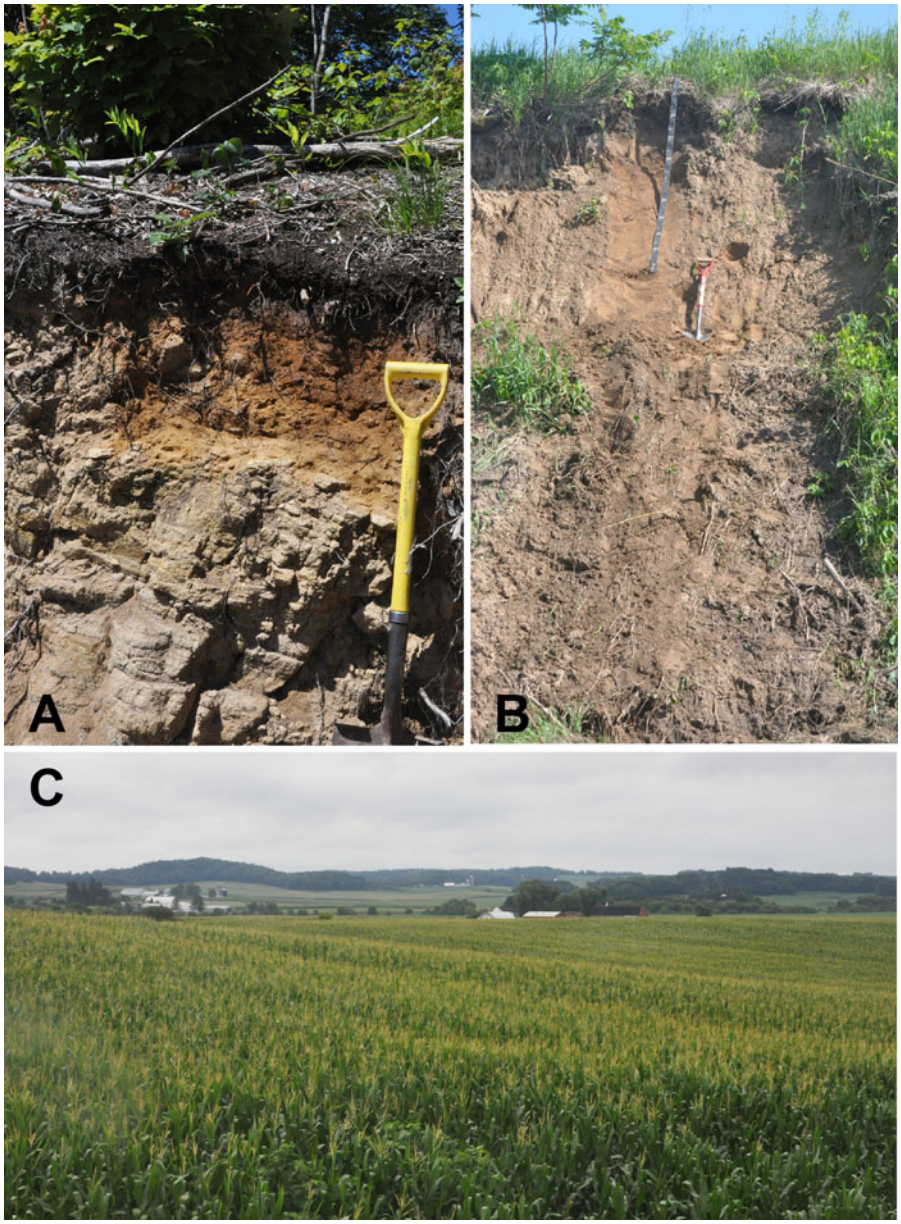


Figure 6. Exposures of rock and sediment on the windward and lee sides of a sandstone upland in the study area. (**A**) A thin veneer of regolith mantles sandstone bedrock on the windward side of the ridge. (**B**) Loess > 5 m thick is exposed at the Geist core site, in the immediate lee of the bedrock ridge (see Fig. 9). Shovel for scale. (**C**) Row-crop agriculture flourishes in the thick loess that lies in the lee of the bedrock ridges in the distance. Photos by the author.

Mississippi River. Upward in the core, this silt-rich zone abruptly ends in a sandy layer at 360 cm depth. All of the loess above this layer is variously sandy, with a particularly sandy zone between 120 and 80 cm depths. Some of this loess has sand contents >30% (Fig. 9). I interpret this 360-cm-thick, upper zone of sandy loess as having formed during a second depositional interval, when saltating sands were commonplace on the landscape. At this time, loess was likely being re-entrained by saltating sand and transported downwind. Periods of particularly strong winds drove enough sand over the ridge to form sandy zones in the upper part of the loess at the Geist site. Spatially, the sand contents in the upper 2 m of loess decrease rapidly downwind from the ridge (Fig. 8B).

Evidence that could point to a second period of loess deposition in the region (and hence, support Scenario 2) has been reported in other studies. In thick loess on uplands in the western part of the study area, Schaetzl et al. (2014) reported that sand contents and modal grain-size values tend to increase nearer the surface. One of these sites (Henning 2) is located on 540 cm of loess, about 100 m southeast of the crest of a ridge. The loess at this site contained considerable amounts of sand, whereas at two other sites on the same ridge (Henning 1 and 3) but ca. 100–300 m farther downwind, the loess lacked a near-surface sandy zone. Instead, the loess here was uniformly silty. The thick loess at the Henning sites is similar to that at the Geist site—sandy at sites near the ridge crest, but with far less sand only slightly farther downwind.

Both the data from the distribution of loess (relative to isolated, sandstone uplands), as well as the increases in sand in the upper parts of the loess deposits in the lee of these uplands, point to an early, initial period of loessfall, followed by an event (driven by saltating sand) during which much of this loess was then redistributed. At this time, additional loess was deposited in protected sites in the lee of bedrock uplands (Figs. 5–8). Areas between the ridges were largely scoured clean of loess, although in some lowlands, thin (<45 cm) deposits of loess remain, probably because

https://doi.org/10.1017/qua.2023.68 Published online by Cambridge University Press

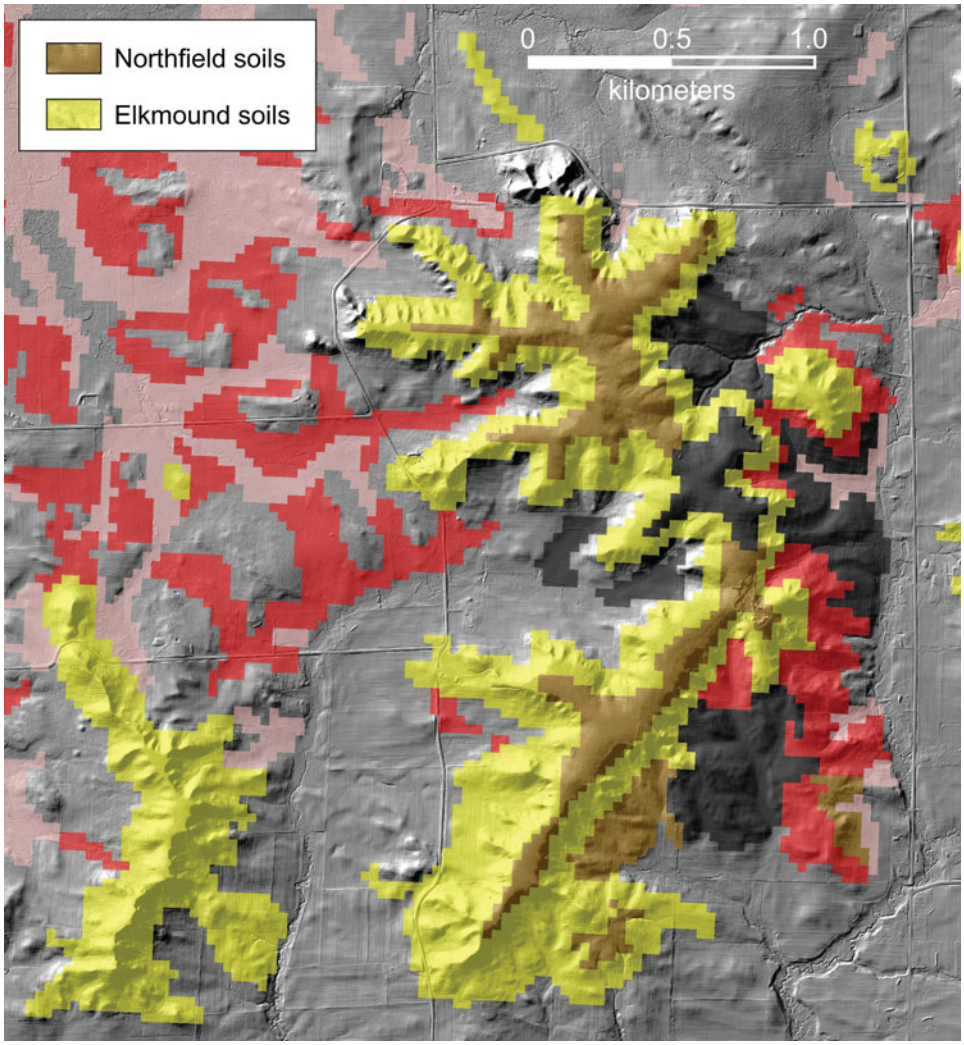


Figure 7. Topography, soils, and loess cover on and near a small, isolated, sandstone ridge (and a smaller, neighboring ridge) in the west-central study area. Soils data from NRCS soil maps.

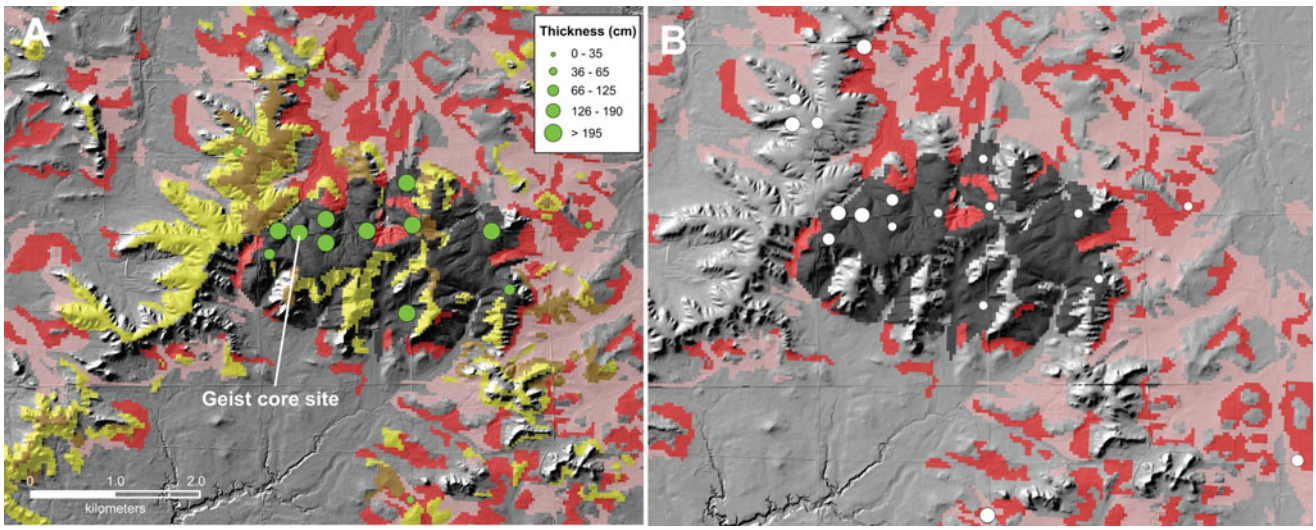


Figure 8. Topography, soils, and loess cover near the Geist core site, on a small, isolated, sandstone ridge in the western part of the study area. Symbology for the loess cover and soils follows that of Fig. 3. Graduated circle maps of loess (**A**) thickness and (**B**) sand content. The data in **B** derive from an amalgamated sample of loess taken by hand auger, and thus reflect the average sand content within that depth interval.

https://doi.org/10.1017/qua.2023.68 Published online by Cambridge University Press

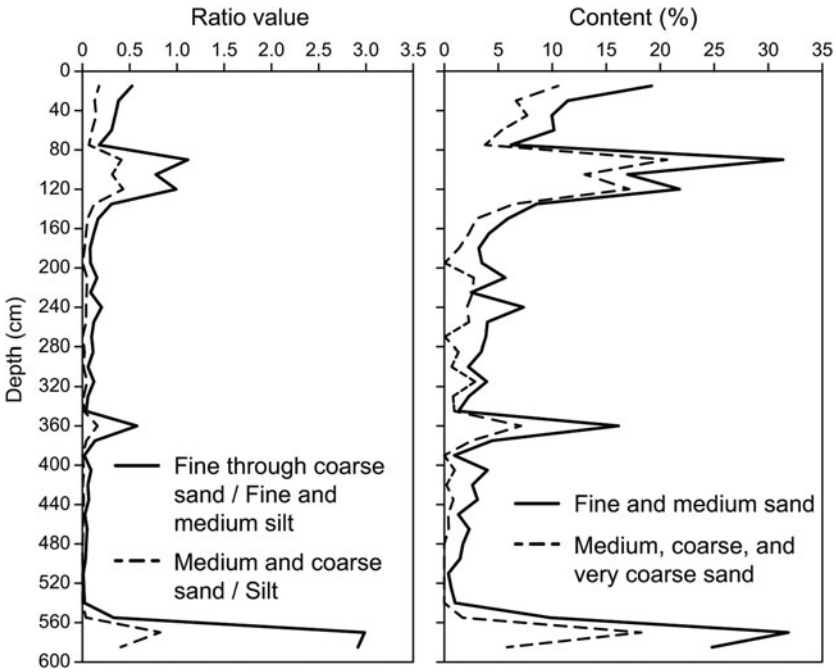


Figure 9. Depth plots of various grain-size fractions and ratios from the Geist site.

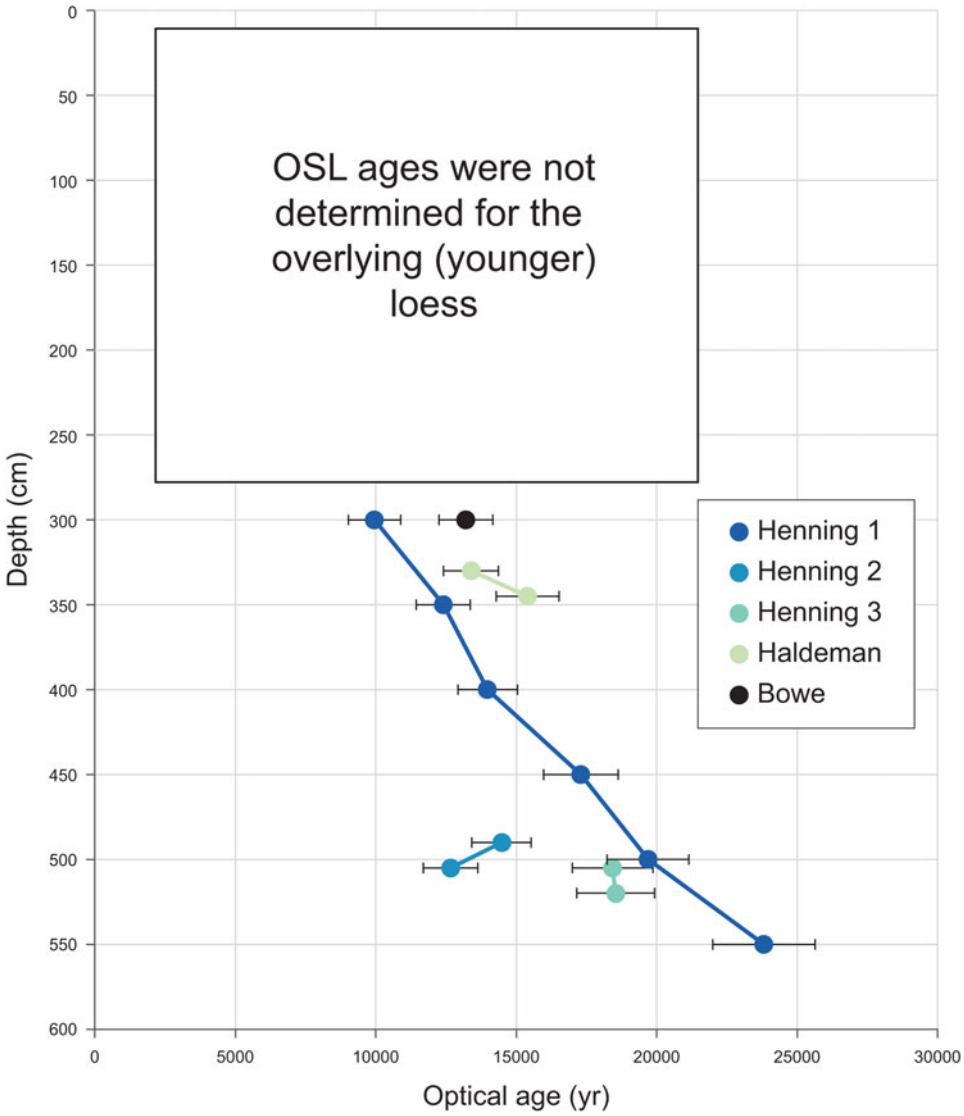


Figure 10. Optically stimulated luminescence (OSL) ages (and their depths) on loess from five sites in the study area, as reported by Schaetzl et al. (2014).

https://doi.org/10.1017/qua.2023.68 Published online by Cambridge University Press

these areas were wet enough to retain a dense vegetation cover. Thus, data from the field tend to support Scenario 2.

Chronology

Sorting out the chronology of loess deposition in the study area could help our understanding of the paleoenvironmental conditions that might have driven the second period of loess erosion and deposition. Only a limited suite of ages exist, however, for what may have been the "first wave" of Peoria loess deposition in western Wisconsin. In their review of loess in the midcontinent, Bettis et al. (2003) reported that Peoria Loess began to accumulate across the Central Lowlands between ca. 23,000 and 22,000 ^{14}C yr BP. For a site near the Mississippi River valley, several tens of kilometers south of the study area, Leigh and Knox (1993) reported a basal age of the Peoria Loess of 24,250 ± 970 yr BP (calibrated to ≈28,365 ± 966 cal yr BP). Within the study area, Schaetzl et al. (2014) reported several optically stimulated luminescence (OSL) ages on loess immediately overlying bedrock ridges in the western part of the study area (Fig. 10). Their data suggest that (initial) loessfall may have begun at some locations in the study area by ca. 24–23 ka. However, the OSL data also suggest that at some sites, loess deposition began much later, ca. 16–13 ka. I suggest that the latter ages represent a second period of loess deposition/remobilization. OSL data from Schaetzl et al. (2014) also suggest that loess continued to accumulate at protected sites for thousands of years, into the Early Holocene.

These data and interpretations support widespread sand and loess remobilization within the study area. The most likely period for such an event would have coincided with cold climatic conditions shortly after the LGM, which in various locations in Wisconsin was between ca. 26 and 21 ka (Carson et al., 2012; Schaetzl et al., 2014), when fresh deposits of outwash sand would have been accumulating within the Chippewa River valley. Considerable evidence also indicates that saltation here was driven by strong WNW winds (Schaetzl et al., 2021), on a permafrost-rich landscape that likely had minimal vegetation cover. Sand wedges in the western part of the study area confirm that saltating sand and permafrost were coincident on this landscape between ca. 19.3 and 14.7 ka, that is, during and shortly after the LGM (Schaetzl et al., 2021). Similar features occur in southeastern Minnesota and northeastern Iowa, west and southwest of the study area (Mason et al., 1992; Walters, 1994). Frequently occurring ventifacts (on quartzite cobbles) on landscapes in and surrounding the study area suggest that the interval of saltating sand was intense and prolonged (Cahow, 1976; Holmes and Syverson, 1997; Johnson, 2000; Schaetzl et al., 2021). Ventifacts and wind-eroded surfaces, which are indicators of paleo-permafrost (Demitroff, 2016), are particularly well developed along the north and south margins of the isolated bedrock uplands. Here, abraded rocks protrude from the land surface, while just a few hundred meters away, directly downwind from the same ridge, thick loess has accumulated (Fig. 11). This pattern suggests that winds were accelerating around the margins of the uplands, as they would have on their ascent up the windward side of the upland. This effect is not unlike what happens at snow fences, where snow drifts form on the lee side of the fence, even as winds are diverted around the ends of the fence.

Thus, it is likely that much of the sand mobilization on the study area landscape may have coincided with a postglacial interval of permafrost (with its minimal vegetation cover) or, as has been documented for similar landscapes in Europe, while the permafrost was thawing (Kasse, 1997; Van Huissteden et al., 2000). Thawing/degrading permafrost here may have led to an overall drier land surface, as infiltration rates and water storage capacities in near-surface sediments increased, facilitating sand mobilization.



Figure 11. Boulders and cobbles—many of them ventifacts—protrude from a wind-eroded surface, a few hundred meters north of a sandstone ridge in the loess transportation surface. Erosion is just as pronounced in the forest, but is not visible in the photo. Thick (>3 m) loess occurs downwind (ESE) of this ridge, less than 1 km from this site. Winds must have been particularly strong around the edges of ridges like this to so effectively abrade the land surface and the rocks. Photo by the author.

https://doi.org/10.1017/qua.2023.68 Published online by Cambridge University Press

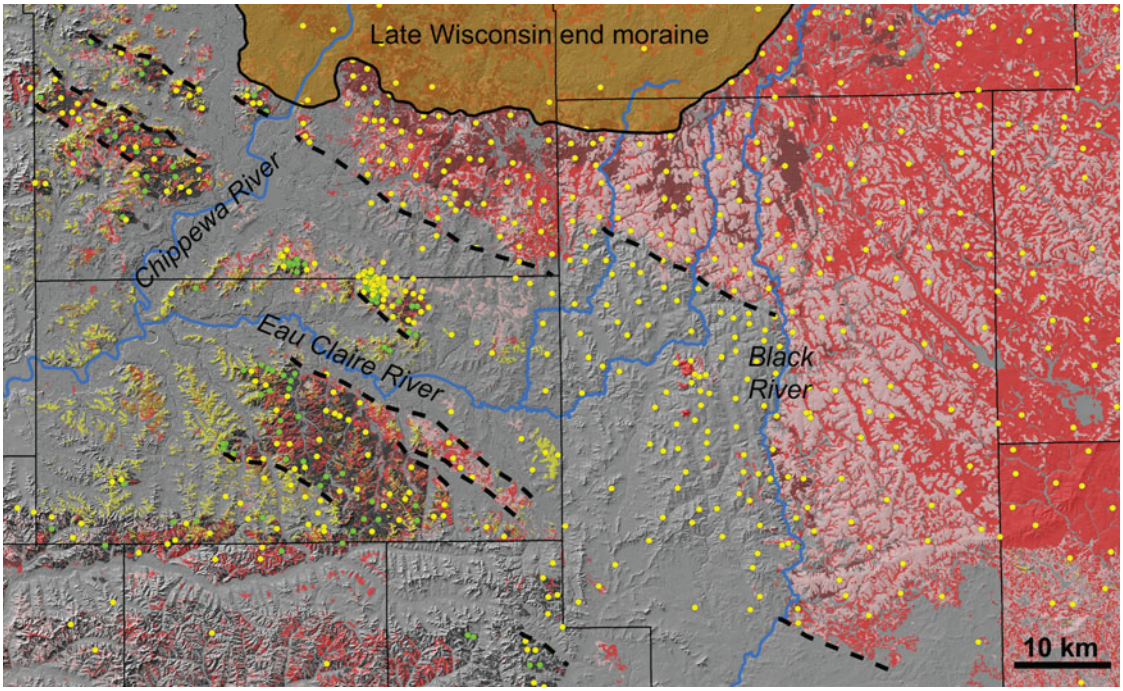


Figure 12. Distribution and thickness of loess, sandy bedrock, and topography across the study area and the loess transportation surface. Dashed lines indicate the noticeably "linear" edges to loess deposits. The symbol legend is similar to that in Fig. 5.

Loess transportation systems II: transport across low-relief landscapes

As discussed earlier, transport of eolian silt across the sandy lowlands of the study area, up, over, and around isolated bedrock uplands, could only have been accomplished by strong winds driving saltating sands across the landscape. This process would have been optimal on low-relief landscapes, where sands are abundant (Figs. 3 and 4). The isolated sandstone uplands discussed earlier are the main topographic obstructions on this otherwise low-relief surface.

Loess in the traditional sense, that is, with silt loam textures, is extremely rare on this transportation surface, as there are few topographic obstructions to shelter it from saltating sands (Fig. 3). Eolian sediment—perhaps remnant deposits of poorly sorted, saltation sand/silt—is present on flatter upland sites, but even there it is so thin and sandy that local soil surveys failed to recognize it (Fig. 7). At almost 30 sites I examined across the transportation surface (all low, upland sites with minimal slope), eolian sediment is absent. Instead, these sites typically have a mantle of sandy loam till or residuum. At six additional sites, the surface sediment was well-sorted, fine, eolian sand.

Initial, broad-based examinations of the loess cover on this transportation surface, as indicated on local soil surveys, reveal several important patterns. First, loess deposits (as mapped in the soil surveys) have distinctly linear "edges" that align along NW-SE or WNW-ESE. Many of these "edges" are in the lee of a topographic obstruction such as a bedrock upland or—interestingly—the Late Wisconsin moraine (Fig. 12). Loess



Figure 13. Images of the Black River in the study area. Photos by the author.

https://doi.org/10.1017/qua.2023.68 Published online by Cambridge University Press

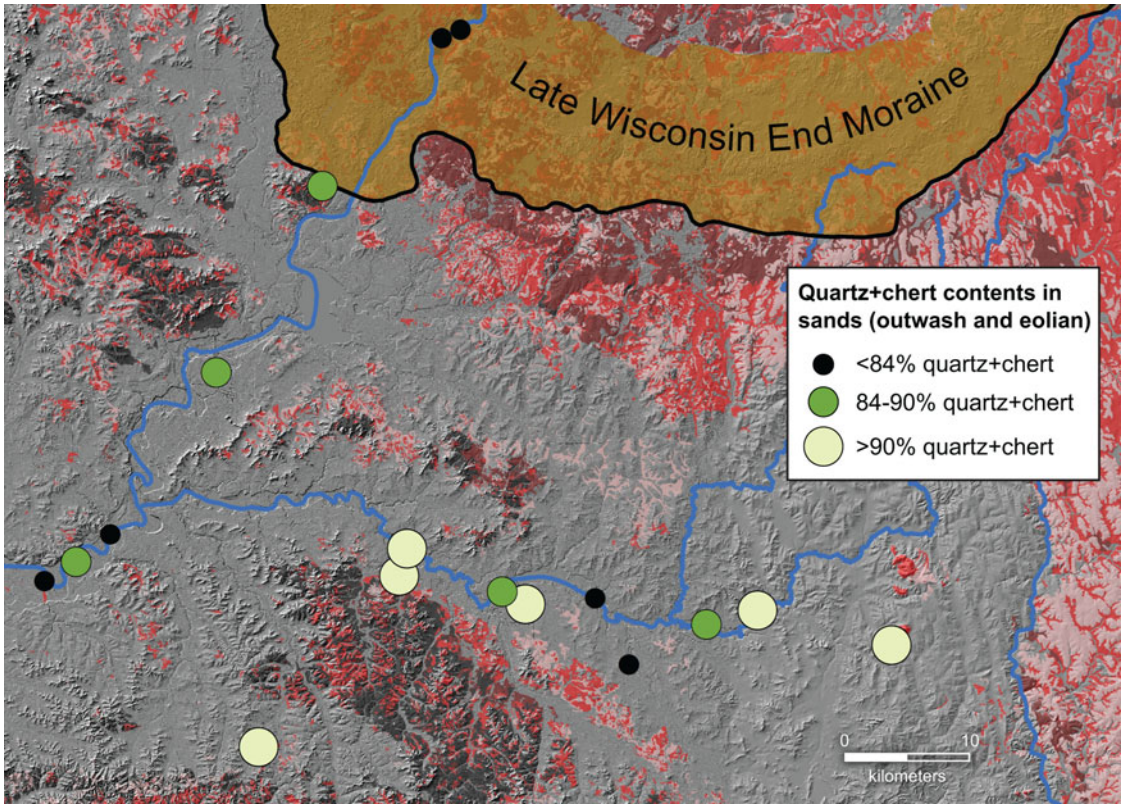


Figure 14. Locations and quantities of quartz and chert in sands from gravel pits and other sandy deposits within the study area.

covers far more of the landscape in the "shadow" of these obstructions (to their east-southeast) than elsewhere on the transportation surface. Like many of the loess deposits, sand stringers to the immediate west of the study area have the same orientation, indicating that winds strong enough to drive saltating sand were most commonly from the NW or WNW (Schaetzl et al., 2018). These patterns indicate that loess can accumulate and/or be protected not only in the lee

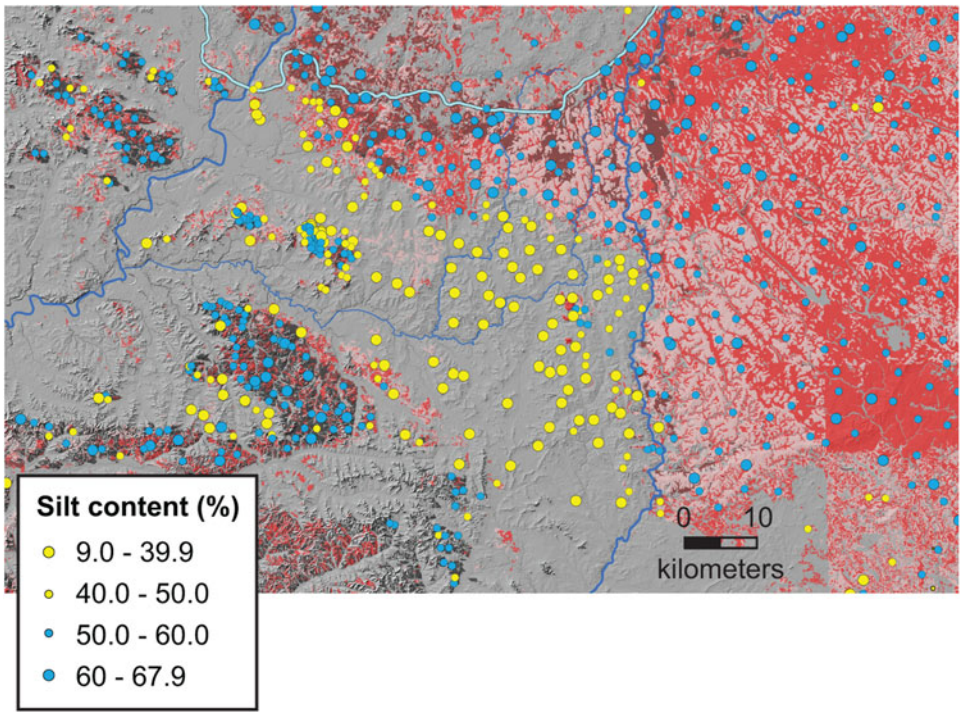


Figure 15. Graduate circle maps of the silt contents of the sampled eolian sediment across the study area. Samples that have sand as the dominant grain-size are shown in yellow; silt-rich samples are in blue.

https://doi.org/10.1017/qua.2023.68 Published online by Cambridge University Press

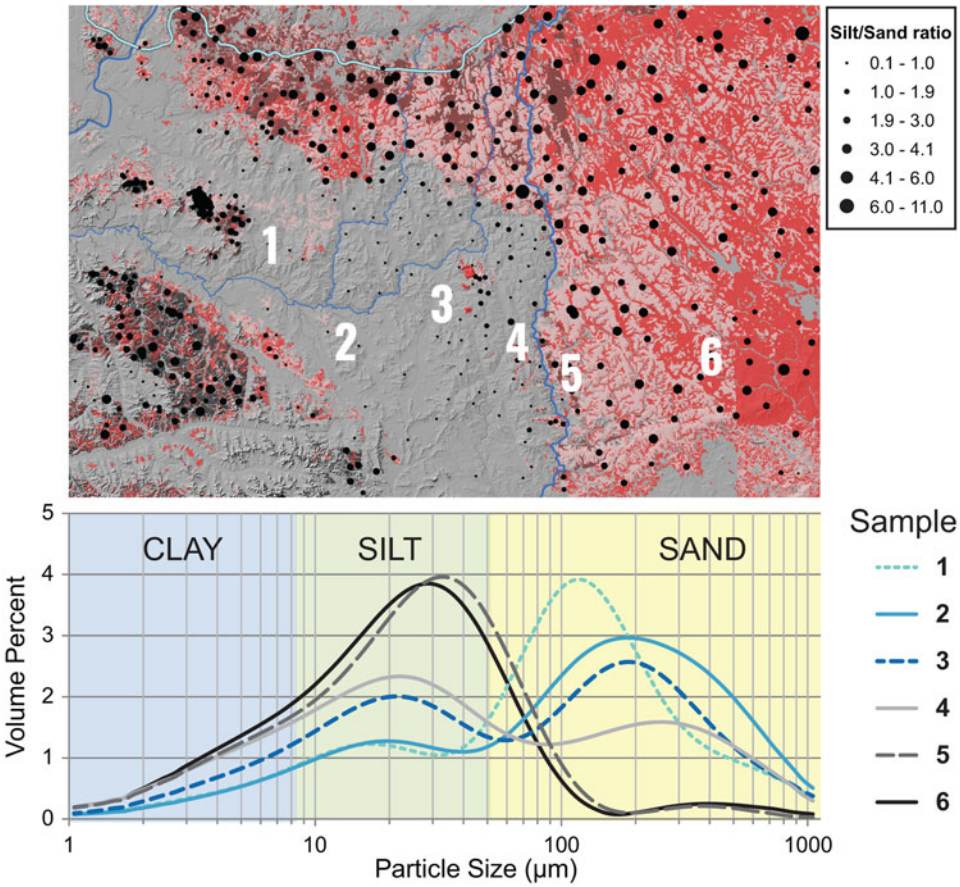


Figure 16. Grain-size curves for six representative samples of eolian sediment across and beyond the loess transportation surface. Graduated sizes of circles on the map depict the ratio of silt/sand within the sediment.

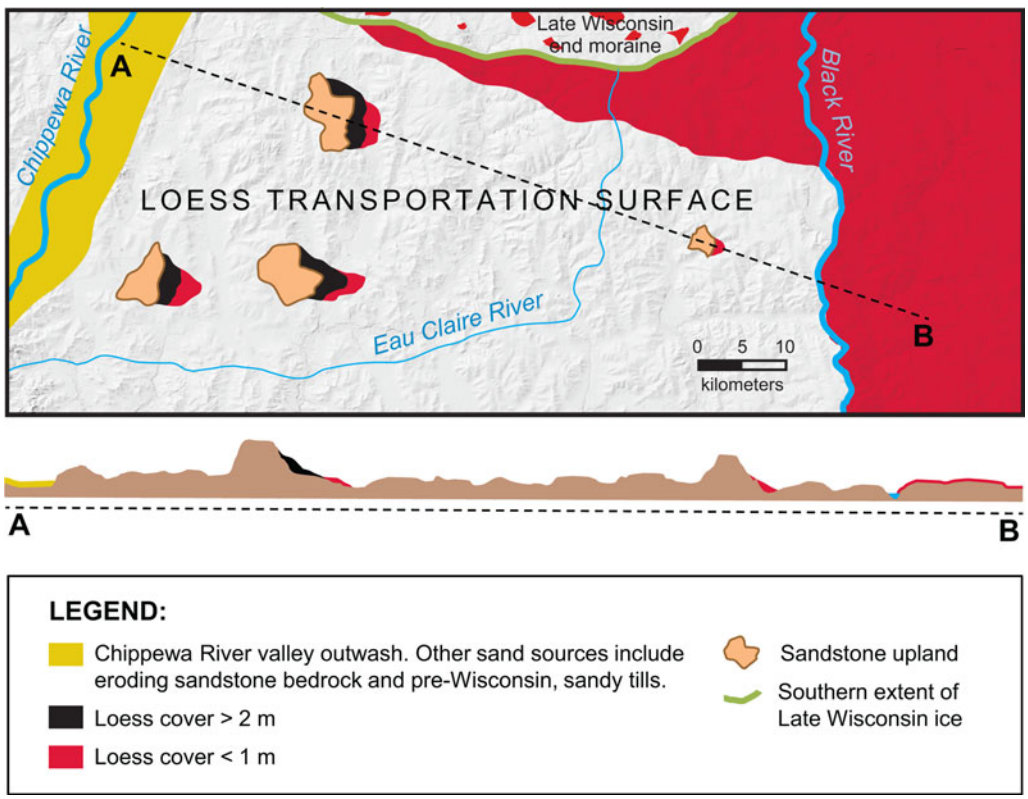


Figure 17. A generalized, summary diagram of the distribution and thickness of loess across the study area, as it pertains to topography and sources of potentially saltating sand. The A-B transect across the landscape is shown as a general topographic and sedimentologic profile in the center of the figure.

https://doi.org/10.1017/qua.2023.68 Published online by Cambridge University Press

of bedrock uplands but in the lee of wide, hummocky moraines —anything that can stop saltating sand.

Although loess deposits are generally absent across the transportation surface, loess *is* widespread downwind (east) of the Black River. Loess here is typically 40–70 cm thick, and often slightly thicker near the river. In contrast, the patchy, poorly sorted eolian sediment within the transportation surface is typically 20–50 cm thick. This pattern fits well with the LTSM of Mason et al. (1999)—saltating sand on the loess transportation surface has deflated silt from this landscape, but because these sands were unable to cross the wide (and in places, deep) valley of the Black River (Figs. 12 and 13), silt-rich loess could accumulate in downwind areas. The sand was largely stopped at the river, just as it was at the isolated sandstone uplands farther to the west, on the same transportation surface. This pattern does not manifest itself relative to the much smaller tributaries of the Eau Claire River, suggesting that sand *was* able to cross these valleys. Thus, the geometry and width of river valleys and other topographic obstructions appears to also figure into the LTSM (Putman et al., 1988).

To further examine the hypothesis that sands were driven across the transportation surface on westerly winds from upwind outwash sources, I sampled (1) gravel pits cut into outwash deposits of the Chippewa River, (2) eolian sands on upland sites on the transportation surface, and (3) fluvial sands within the Eau Claire River valley. The data indicate that the sands within the Chippewa River valley are commonly enriched in "heavy" minerals, whereas sands are much more quartz-rich on the transportation surface (Fig. 14). This pattern supports the model of eolian transport of sands across the loess transportation surface, such that the lightest minerals became enriched en route.

Finally, I performed a more detailed examination of sand and silt contents of eolian sediments across the study area, and on the transportation surface in particular, to further verify the efficacy of the LTSM (Fig. 15). The sediments on the transportation surface, which are assumedly reflective of the sediment as it crossed the landscape, are dominated by fine and very fine sand and have low (but not insignificant) contents of silt (Fig. 16). As expected, silt contents on the transportation surface are much higher at sites downwind of isolated bedrock ridges. Mean weighted particle size (MWPS) data (not shown) confirm these predictable spatial patterns; eolian samples on the transportation surface have high MWPS values, which decline abruptly across the Black River and in areas downwind of bedrock uplands. Notably, upland sites north of the transportation surface but south of the end moraine are covered with silt-rich loess. This area was protected from saltating sand being driven by NW and WNW winds, and hence, silt-rich loess was retained on the landscape.

CONCLUSIONS

The theory behind a loess transportation surface, first introduced by Mason et al. (1999), can often be used to explain the thickness, texture, and patchy distribution of various kinds of eolian sediments, particularly loess. In the immediate postglacial period, west-central Wisconsin had all the essential components necessary for loess destabilization and transportation—abundant sands from a variety of sources; an interval in the geologic past with cold, windy cold conditions and (likely) minimal vegetation cover due to permafrost; and loess that was either being brought in as dust in suspension or was already present on the landscape. South of the study area, loess transportation surfaces are less common, probably because of a denser vegetation cover that precluded the generation of large amounts of saltating sand (Mason et al., 1999). Today, the western Wisconsin study area has only patchy loess cover, with most of the loess (and the thickest deposits) occurring in areas that were protected from saltating sands that were being driven on strong westerly and northwesterly winds. Loess is generally absent from sites exposed to those saltating sands. Loess deposits are present, and often quite thick, at protected sites, such as those in the lee of (1) the Black River valley and (2) large, isolated bedrock uplands. Even the Late Wisconsin moraine was generally able to protect the landscape to its southeast from deflation of silt by saltating sand, resulting in a loess cover in its lee (Fig. 17). The moraine, the Black River, and the bedrock uplands were all able to stop or hinder the effects of saltating sand, while allowing silt in suspension to continue on, downwind. The presence of thick loess deposits in the lee of these uplands, combined with evidence of intense eolian erosion around their windward margins, portends that the winds were very strong at this time. Evidence also exists for an early period of dust deposition from distant, westerly sources, followed by a period (ca. 16–13 ka) when much of this loess may have then been re-entrained and deposited farther downwind, in protected sites. This later loess often is slightly sandier.

In summary, this work supports the contention of Mason et al. (1999, p. 223) that loess has "a critical but indirect role in the regional spatial pattern of loess transport and deposition through its effect on the movement of saltating sand." Across my study area, loess transportation surfaces take two forms: (1) an extensive, low-relief landscape with only scattered patches of silty-sandy eolian sediment, mainly on broad uplands; and (2) the windward slopes of bedrock uplands, which may even have acted as sand ramps.

Acknowledgments. The hundreds of samples that form the backbone of this study were collected over several years with the help of numerous colleagues, friends, and students. Some of the samples were part of Kristy Gruley's master's thesis. Pete Scull, David Schaetzl, John Attig, and Greg Hamann also assisted with field sampling. Garry Running, Phil Larson, Doug Faulkner, and their students from UW–Eau Claire did the coring at the Geist site. I am grateful to many landowners who allowed me to do extensive sampling on their land, particularly Joann and Roger Henning, Kris Brown, and Wayne Geist. Ha-Jin Kim assisted with the graphics, Andy Finley analyzed the grain-size data for modal values, and Chris Baish helped with quality-control checks on the large data sets involved in a study like this. Finally, I am grateful to Joe and Christina Hupy for their hospitality—housing me (many times) while I was in the field. Two anonymous reviewers were of great help in review and revision stages of this project.

REFERENCES

Amit, R., Enzel, Y., Mushkin, A., Gillespie, A., Batbaatar, J., Crouvi, O., Vandenberghe, J., An, Z., 2014. Linking coarse silt production in Asian sand deserts and Quaternary accretion of the Chinese Loess Plateau. *Geology* **42**, 23–26.

Assallay, A.M., Rogers, C.D.F., Smalley, I.J., Jefferson, I.F., 1998. Silt: 2-62 um, 9-4 φ. *Earth-Science Reviews* **45**, 61–88.

Attig, J.W., Bricknell, M., Carson, E.C., Clayton, L., Johnson, M.D., Mickelson, D.M., Syverson, K.M., 2011. *Glaciation of Wisconsin*. 4th ed. Wisconsin Geological and Natural History Survey Educational Series Publication 36. Wisconsin Geological and Natural History Survey, Madison.

Attig, J.W., Clayton, L., 1993. Stratigraphy and origin of an area of hummocky glacial topography, northern Wisconsin, U.S.A. *Quaternary International* **18**, 61–67.

Attig, J.W., Muldoon, M.A., 1989. *Pleistocene Geology of Marathon County, Wisconsin*. Wisconsin Geological and Natural History Survey Information

https://doi.org/10.1017/qua.2023.68 Published online by Cambridge University Press

Circular 65. University of Wisconsin-Extension, Geological and Natural History Survey, Madison.

Bagnold, R.A., 1941. *The Physics of Blown Sand and Desert Dunes*. Methuen, London.

Batchelor, C.J., Orland, I.J., Marcott, S.A., Slaughter, R., Edwards, R.L., Zhang, P., Li, X., Cheng, H., 2019. Distinct permafrost conditions across the last two glacial periods in midlatitude North America. *Geophysical Research Letters* **46**, 13318–13326.

Bertran, P., Bosq, M., Boderie, Q., Coussot, C., Coutard, S., Deschodt, L., Franc, O., Gardere, P., Liard, M., Wuscher, P., 2021. Revised map of European aeolian deposits derived from soil texture data. *Quaternary Science Reviews* **266**, 107085.

Bettis, E.A. III, Muhs, D.R., Roberts, H.M., Wintle, A.G., 2003. Last glacial loess in the conterminous USA. *Quaternary Science Reviews* **22**, 1907–1946.

Bromwich, D.H., Toracinta, E.R., Wei, H., Oglesby, R.J., Fastook, J.L., Hughes, T.J., 2004. Polar MM5 simulations of the winter climate of the Laurentide Ice Sheet at the LGM. *Journal of Climate* **17**, 3415–3433.

Cahow, A.C., 1976. *Glacial Geomorphology of the Southwestern Segment of the Chippewa Lobe Moraine Complex, Wisconsin*. PhD dissertation, Michigan State University, East Lansing.

Carson, E.C., Hanson, P.R., Attig, J.W., Young, A.R., 2012. Numeric control on the late-glacial chronology of the southern Laurentide Ice Sheet derived from ice-proximal lacustrine deposits. *Quaternary Research* **78**, 583–589.

Clayton, L., 1991. *Pleistocene Geology of Wood County, Wisconsin*. Wisconsin Geological and Natural History Survey Information Circular 68. University of Wisconsin-Extension, Geological and Natural History Survey, Madison.

Clayton, L., Attig, J.W., Mickelson, D.M., 2001. Effects of late Pleistocene permafrost on the landscape of Wisconsin, USA. *Boreas* **30**, 173–188.

COHMAP Members, 1988. Climatic changes of the last 18,000 years: observations and model simulations. *Science* **241**, 1043–1052.

Conroy, J.L., Karamperidou, C., Grimley, D.A., Guenthe, W.R., 2019. Surface winds across eastern and midcontinental North America during the Last Glacial Maximum: a new data-model assessment. *Quaternary Science Reviews* **220**, 14–29.

Demitroff, M., 2016. Pleistocene ventifacts and ice-marginal conditions, New Jersey, USA. *Permafrost and Periglacial Processes* **27**, 123–137.

Faulkner, D.J., Larson, P.H., Jol, H.M., Running, G.L., Loope, H.M., Goble, R.J., 2016. Autogenic incision and terrace formation resulting from abrupt late-glacial base-level fall, lower Chippewa River, Wisconsin, USA. *Geomorphology* **266**, 75–95.

Fehrenbacher, J.B., White, J.L., Ulrich, H.P., Odell, R.T., 1965. Loess distribution in southeastern Illinois and southwestern Indiana. *Soil Science Society of America Proceedings* **29**, 566–572.

Frazee, C.J., Fehrenbacher, J.B., Krumbein, W.C., 1970. Loess distribution from a source. *Soil Science Society of America Proceedings* **34**, 296–301.

French, H.M., Millar, S.W.S., 2014. Permafrost at the time of the Last Glacial Maximum (LGM) in North America. *Boreas* **43**, 667–677.

Gardner, R.A.M., Rendell, H.M., 1994. Loess, climate and orogenesis: implications of South Asian loesses. *Zeitschrift für Geomorphologie* **2**, 169–184.

Hallberg, G.R., 1979. Wind-aligned drainage in loess in Iowa. *Proceedings of the Iowa Academy of Science* **86**, 4–9.

Hanson, P., Mason, J., Jacobs, P., Young, A., 2015. Evidence for bioturbation of luminescence signals in eolian sand on upland ridgetops, southeastern Minnesota, USA. *Quaternary International* **362**, 108–115.

Hole, F.D., 1943. Correlation of the glacial border drift of north central Wisconsin. *American Journal of Science* **241**, 498–516.

Hole, F.D., 1950 (repr. 1968). *Aeolian Sand and Silt Deposits of Wisconsin*. Wisconsin Geological and Natural History Survey Map. University of Wisconsin-Extension, Geological and Natural History Survey, Madison.

Holmes, M.A., Syverson, K.M., 1997. Permafrost history of Eau Claire and Chippewa Counties, Wisconsin, as indicated by ice-wedge casts. *The Compass* **73**, 91–96.

Jacobs, P.M., Mason, J.A., Hanson, P.R., 2011. Mississippi Valley regional source of loess on the southern Green Bay Lobe land surface, Wisconsin. *Quaternary Research* **75**, 574–583.

Jacobs, P.M., Mason, J.A., Hanson, P.R., 2012. Loess mantle spatial variability and soil horizonation, southern Wisconsin, USA. *Quaternary International* **265**, 42–53.

Johnson, M.D., 1986. *Pleistocene Geology of Barron County, Wisconsin*. Wisconsin Geological and Natural History Survey Information Circular 55. University of Wisconsin-Extension, Geological and Natural History Survey, Madison.

Johnson, M.D., 2000. *Pleistocene Geology of Polk County, Wisconsin*. Wisconsin Geological and Natural History Survey Bulletin 95. University of Wisconsin-Extension, Geological and Natural History Survey, Madison.

Kasse, C., 1997. Cold-climate aeolian sand-sheet formation in North-Western Europe (c. 14–12.4 ka): a response to permafrost degradation and increased aridity. *Permafrost and Periglacial Processes* **8**, 295–311.

Kerr, P.J., 2023. *A Late Wisconsin polygenetic landscape: connecting landforms on the Iowan erosion surface to past processes with LiDAR and field data*. INQUA Conference, Rome, Italy, abstract.

Krist, F., Schaetzl, R.J., 2001. Paleowind (11,000 BP) directions derived from lake spits in northern Michigan. *Geomorphology* **38**, 1–18.

Kutzbach, J.E., Guetter, P.J., Behling, P.J., Selin, R., 1993. Simulated climatic changes: results of the COHMAP climate-model experiments. In: Wright, H.E. Jr., Kutzbach, J.E., Webb, T. III, Ruddiman, W.F., Street-Perrott, F.A., Bartlein P.J. (Eds.), *Global Climates since the Last Glacial Maximum*. University of Minnesota Press, Minneapolis, pp. 24–93.

Leigh, D.S., Knox, J.C., 1993. AMS radiocarbon age of the Upper Mississippi Valley Roxana Silt. *Quaternary Research* **39**, 282–289.

Leighton, M.M., Willman, H.B., 1950. Loess formations of the Mississippi Valley. *Journal of Geology* **58**, 599–623.

Li, Y., Shi, W., Aydin, A., Beroya-Eitner, M.A., Gao, G., 2020. Loess genesis and worldwide distribution. *Earth-Science Reviews* **201**, 102947.

Loope, W.L., Loope, H.M., Goble, R.J., Fisher, T.G., Lytle, D.E., Legg, R.J., Wysocki, D.A., Hanson, P.R., Young, A.R., 2012. Drought drove forest decline and dune building in eastern USA, as the upper Great Lakes became closed basins. *Geology* **40**, 315–318.

Luehmann, M.D., Peter, B., Connallon, C.B., Schaetzl, R.J., Smidt, S.J., Liu, W., Kincare, K., Walkowiak, T.A., Thorlund, E., Holler, M.S., 2016. Loamy, two-storied soils on the outwash plains of southwestern Lower Michigan: pedoturbation of loess with the underlying sand. *Annals of the American Association of Geographers* **106**, 551–571.

Luehmann, M.D., Schaetzl, R.J., Miller, B.A., Bigsby, M., 2013. Thin, pedoturbated and locally sourced loess in the western Upper Peninsula of Michigan. *Aeolian Research* **8**, 85–100.

Mason, J.A., 2001. Transport direction of Peoria loess in Nebraska and implications for loess source areas on the central Great Plains. *Quaternary Research* **56**, 79–86.

Mason, J.A., Jacobs, P.M., Leigh, D.S., 2019. Loess, eolian sand, and colluvium in the Driftless Area. *Geological Society of America, Special Paper* **543**, 61–73.

Mason, J.A., Nater, E.A., Bell, J.C., Hobbs, J.C., 1992. Use of ice-wedge casts to establish the relative age of soils and geomorphic surfaces in the Upper Midwest. *Soil Science Society of America, Annual Meeting Abstracts*.

Mason, J.A., Nater, E.A., Hobbs, H.C., 1994. Transport direction of Wisconsinan loess in southeastern Minnesota. *Quaternary Research* **41**, 44–51.

Mason, J.A., Nater, E.A., Zanner, C.W., Bell, J.C., 1999. A new model of topographic effects on the distribution of loess. *Geomorphology* **28**, 223–236.

Mason, J.A., Swinehart, J.B., Hanson, P.R., Loope, D.B., Goble, R.J., Miao, X., Schmeisser, R.L., 2011. Late Pleistocene dune activity in the central Great Plains, USA. *Quaternary Science Reviews* **30**, 3858–3870.

McSweeney, K., Leigh, D.S., Knox, J.C., Darmody, R.H., 1988. Micromorphological analysis of mixed zones associated with loess deposits of the midcontinental United States. In: Eden, D.N., Furkert, R.J. (Eds.), *Loess: Its Distribution, Geology and Soils. Proceedings of an International Symposium, New Zealand, 13–21 February 1987*. Balkema, Rotterdam, pp. 117–130.

Miller, B.A., Schaetzl, R.J., 2012. Precision of soil particle size analysis using laser diffractometry. *Soil Science Society of America Journal* **76**, 1719–1727.

Mode, W.N., 1976. The Glacial Geology of a Portion of North-Central Wisconsin. M.S. thesis, University of Wisconsin–Madison.

https://doi.org/10.1017/qua.2023.68 Published online by Cambridge University Press

Mudrey, M.G., Brown, B.A., Greenberg, J.K., 1982. *Bedrock Geologic Map of Wisconsin*. University of Wisconsin-Extension, Geological and Natural History Survey, Madison.

Muhs, D.R., Bettis, E.A. III, 2000. Geochemical variations in Peoria loess of western Iowa indicate paleowinds of midcontinental North America during last glaciation. *Quaternary Research* **53**, 49–61.

Muhs, D.R., Bettis, E.A. III, Roberts, H.M., Harlan, S.S., Paces, J.B., Reynolds, R.L., 2013. Chronology and provenance of last-glacial (Peoria) loess in western Iowa and paleoclimatic implications. *Quaternary Research* **80**, 468–481.

Muhs, D.R., Bettis, E.A., Skipp, G.L., 2018. Geochemistry and mineralogy of late Quaternary loess in the upper Mississippi River valley, USA: provenance and correlation with Laurentide ice sheet history. *Quaternary Science Reviews* **187**, 235–269.

Nickling, W.G., 1978. Eolian sediment transport during dust storms: Slims River Valley, Yukon Territory. *Canadian Journal of Earth Sciences* **15**, 1069–1084.

Nyland, K.E., Schaetzl, R.J., Ignatov, A., Miller, B.A., 2018. A new depositional model for sand-rich loess on the Buckley Flats outwash plain, northwestern Lower Michigan. *Aeolian Research* **31**, 91–104.

Olson, C.G., Ruhe, R.V., 1979. Loess dispersion model, southwest Indiana, U.S.A. *Acta Geologica Academiae Scientiarum Hungaricae, Tomus* **22**, 205–227.

Pötter, S., Veres, D., Baykal, Y., Nett, J.J., Schulte, P., Hambach, U., Lehmkuhl, F., 2021. Disentangling sedimentary pathways for the Peniglacial Lower Danube Loess based on geochemical signatures. *Frontiers in Earth Science* **9**, 600010.

Putman, B.R., Jansen, I.J., Follmer, L.R., 1988. Loessial soils: their relationship to width of the source valley in Illinois. *Soil Science* **146**, 241–247.

Roberts, H.M., Muhs, D.R., Wintle, A.G., Duller, G.A.T., Bettis, E.A. III, 2003. Unprecedented last-glacial mass accumulation rates determined by luminescence dating of loess from western Nebraska. *Quaternary Research* **59**, 411–419.

Ruhe, R.V., 1973. Background of model for loess-derived soils in the upper Mississippi Valley. *Soil Science* **115**, 250–253.

Ruhe, R.V., 1984. Loess derived soils, Mississippi valley region: I. Soil sedimentation system. *Soil Science Society of America Journal* **48**, 859–867.

Rutledge, E.M., Holowaychuk, N., Hall, G.F., Wilding, L.P., 1975. Loess in Ohio in relation to several possible source areas: I. Physical and chemical properties. *Soil Science Society of America Proceedings* **39**, 1125–1132.

Schaetzl, R.J., Attig, J.W., 2013. The loess cover of northeastern Wisconsin. *Quaternary Research* **79**, 199–214.

Schaetzl, R.J., Forman, S.L., Attig, J.W., 2014. Optical ages on loess derived from outwash surfaces constrain the advance of the Laurentide Ice Sheet out of the Lake Superior Basin, USA. *Quaternary Research* **81**, 318–329.

Schaetzl, R.J., Hook, J., 2008. Characterizing the silty sediments of the Buckley Flats outwash plain: evidence for loess in NW Lower Michigan. *Physical Geography* **29**, 1 18.

Schaetzl, R.J., Krist, F.J. Jr., Luehmann, M.D. Lewis, C.F.M., Michalek, M.J., 2016. Spits formed in Glacial Lake Algonquin indicate strong easterly winds over the Laurentide Great Lakes during Late Pleistocene. *Journal of Paleolimnology* **55**, 49–65.

Schaetzl, R.J., Larson, P.H., Faulkner, D.J., Running, G.L., Jol, H.M., Rittenour, T.M., 2018. Eolian sand and loess deposits indicate west-northwest paleowinds during the Late Pleistocene in Western Wisconsin, USA. *Quaternary Research* **89**, 769–785.

Schaetzl, R.J., Luehmann, M.D., 2013. Coarse-textured basal zones in thin loess deposits: products of sediment mixing and/or paleoenvironmental change? *Geoderma* **192**, 277–285.

Schaetzl, R.J., Nyland, K.E., Kasmerchak, C.S., Breeze, V., Kamoske, A., Thomas, S.E., Bomber, M., Grove, L., Komoto, K., Miller, B.A., 2021. Holocene, silty-sand loess immediately downwind of dunes in northern Michigan, USA. *Physical Geography* **42**, 25–29.

Schaetzl, R.J., Running, G. IV, Larson, P., Rittenour, T., Yansa, C., Faulkner, D., 2022. Luminescence dating of sand wedges constrains the Late Wisconsin (MIS-2) permafrost interval in the Upper Midwest, USA. *Boreas* **51**, 385–401.

Scull, P., Schaetzl, R.J., 2011. Using PCA to characterize and differentiate the character of loess deposits in Wisconsin and Upper Michigan, USA. *Geomorphology* **127**, 143–155.

Shandonay, K.L., Bowen, M.W., Larson, P.H., Running, G.L., Rittenour, T., Mataitis, R., 2022. Morphology and stratigraphy of aeolian sand stringers in southeast Minnesota and western Wisconsin, USA. *Earth Surface Processes and Landforms* **47**, 2863–2876.

Smalley, I.J., 1966. The properties of glacial loess and the formation of loess deposits. *Journal of Sedimentary Petrology* **36**, 669–676.

Smalley, I.J., Vita Finzi, C., 1968. The formation of fine particles in sandy deserts and the nature of "desert" loess. *Journal of Sedimentary Petrology* **38**, 766 774.

Smith, B.J., Wright, J.S., Whalley, W.B., 2002. Sources of non-glacial, loess-size quartz silt and the origins of "desert loess." *Earth-Science Reviews* **59**, 1–26.

Smith, G.D., 1942. *Illinois Loess: Variations in Its Properties and Distribution*. University of Illinois Agricultural Experiment Station, Bulletin 490. University of Illinois, Agricultural Experiment Station, Urbana-Champaign.

Stevens, T., Sechi, D., Tziavaras, C., Schneider, R., Banak, A., Andreucci, S., Hattestrand, M., Pascucci, V., 2022. Age, formation and significance of loess deposits in central Sweden. *Earth Surface Processes and Landforms* **47**, 3276–3301.

Stewart, M.T., 1973. Pre-Woodfordian Drifts of North-Central Wisconsin. M.S. thesis, University of Wisconsin–Madison.

Stewart, M.T., Mickelson, D.M., 1976. Clay mineralogy and relative ages of tills in north-central Wisconsin. *Journal of Sedimentary Petrology* **46**, 200–205.

Sweeney, M.R., Busacca, A.J., Gaylord, D.R., Gaylord, A., 2005. Topographic and climatic influences on accelerated loess accumulation since the last glacial maximum in the Palouse, Pacific Northwest, USA. *Quaternary Research* **63**, 261–273.

Sweeney, M.R., Mason, J.A., 2013. Mechanisms of dust emission from Pleistocene loess deposits, Nebraska, USA. *Journal of Geophysical Research: Earth Surface* **118**, 1460–1471.

Syverson, K.M., 2007. *Pleistocene Geology of Chippewa County, Wisconsin*. Wisconsin Geological and Natural History Survey Bulletin 103. University of Wisconsin-Extension, Geological and Natural History Survey, Madison.

Syverson, K.M., Colgan, P.M., 2011. The Quaternary of Wisconsin: an updated review of stratigraphy, glacial history, and landforms. In: Ehlers, J., Gibbard, P.L., Hughes, P.D. (Eds.), *Quaternary Glaciations—Extent and Chronology*. Part IV, *A Closer Look*. Elsevier, Amsterdam, pp. 537–552.

Thomas, D.D., 1977. *Soil Survey of Eau Claire County, Wisconsin*. Soil Conservation Service, U.S. Government Printing Office, Washington, DC.

Van Huissteden, J.K., Vandenberghe, J., Van der Hammen, T., Laan, W., 2000. Fluvial and aeolian interaction under permafrost conditions: Weischselian Late Pleniglacial, Twente, eastern Netherlands. *Catena* **40**, 307–321.

Vanmaercke-Gottigny, M.C., 1981. Some geomorphological implications of the cryo-aeolian deposits in western Belgium. *Biuletyn periglacial* **28**, 103–114.

Walters, J.C., 1994. Ice-wedge casts and relict polygonal ground in north-east Iowa, USA. *Permafrost and Periglacial Processes* **5**, 269–282.

Wang, Z.Y., Wu, Y.Q., Li, D.W., Fu, T.Y., 2022. The southern boundary of the Mu Su Sand Sea and its controlling factors. *Geomorphology* **396**, 108010.

Waroszewski, J., Sprafke, T., Kabala, C., Kobierski, M., Kierczak, J., Musztyfaga, E., Loba, A., Mazurek, R., Labaz, B., 2019. Tracking textural, mineralogical and geochemical signatures in soils developed from basalt-derived materials covered with loess sediments (SW Poland). *Geoderma* **337**, 983–997.

Waroszewski, J., Sprafke, T., Kabala, C., Musztyfaga, E., Łabaz, B., 2017. Aeolian silt contribution to soils on mountain slopes (Mt. Ślęża, SW Poland). *Quaternary Research* **89**, 1–16.

https://doi.org/10.1017/qua.2023.68 Published online by Cambridge University Press